Charging of single Si nanocrystals by atomic force microscopy

E. A. Boer, L. D. Bell,[a] M. L. Brongersma, and H. A. Atwater
Thomas J. Watson Laboratory of Applied Physics, California Institute of Technology, Pasadena, California 91125

M. L. Ostraat and R. C. Flagan
Department of Chemical Engineering, California Institute of Technology, Pasadena, California 91125

(Received 18 December 2000; accepted for publication 19 March 2001)

Conducting-tip atomic force microscopy (AFM) has been used to electronically probe silicon nanocrystals on an insulating substrate. The nanocrystal samples were produced by aerosol techniques and size classified; nanocrystal size can be controlled in the size range of 2–50 nm with a size variation of less than 10%. Using a conducting tip, the charge was injected directly into the nanocrystals, and the subsequent dissipation of the charge was monitored. Estimates of the injected charge can be made by comparison of the data with an intermittent contact mode model of the AFM response to the electrostatic force produced by the stored charge. © *2001 American Institute of Physics.* [DOI: 10.1063/1.1371783]

The expanding capabilities for nanoscale fabrication have spurred interest in single electron transistors and memory devices. While the size regime of most interest for exploitation of single-electron effects is below the resolution threshold for electron-beam lithography, techniques involving self-assembly or nucleation show promise for the creation of ultrasmall device structures. However, practical devices have been limited by issues of size uniformity and spatial ordering of nanoscale features.

Floating gate nonvolatile memories (NVMs) are one of the most accessible applications for room temperature single-electron devices. An intermediate step towards the realization of single-electron NVMs is the replacement of the relatively large, conventional floating gate with a two-dimensional array of small, isolated nanoscale floating gates embedded in the gate oxide. Such structures have been demonstrated[1–4] using Si nanocrystals (NCs) in a conventional floating gate memory configuration. Most commonly these NCs are formed within a SiO_2 layer by implantation and annealing[4] or spontaneous decomposition during chemical vapor deposition.[3] This technique produces an array of NCs with statistical size and position distributions. The devices also exhibit a distribution of charge transit times during charging of an ensemble of nanocrystals. The physical reasons for this behavior are not completely understood, but could be related to a dispersion in thickness of the oxide barrier between the NCs and substrate, interface states in the NCs, or shifts in electronic levels or charging energies due to NC size variations.

Although NCs in NVM elements are buried within an oxide layer, it is also important to characterize the properties of isolated single nanocrystals. The NCs studied in this work were fabricated using a recently developed method for producing size-classified Si nanocrystals.[5] This method enables size classification with a standard deviation of less than 10% and NC sizes as small as 2 nm. The NCs were synthesized by decomposition of silane in a nitrogen carrier gas.[6] Parameters can be adjusted to produce an ultrafine aerosol of single, nonagglomerated particles in the 2–50 nm size range. The aerosol was charged by exposure to ambipolar gas ions, and size classification was accomplished by a radial differential mobility analyzer.[5] Nanocrystals were collected on an oxidized Si substrate by electrostatic precipitation. Substrate oxide thickness was 100 nm.

In order to understand the electronic properties on a single-NC level, atomic force microscopy (AFM)[7] was performed with a conducting tip[8] to probe individual Si nanocrystals. AFM can be performed either in contact mode or in intermittent contact (tapping) mode.[9] The energy transfer to the sample surface is smaller in tapping mode, and the average tip-sample spacing is larger. Tapping mode operation is effective for imaging without moving objects, since sampling by the tip is pointwise, while contact mode can be used for surface modification and manipulation. Manipulation of GaAs[10] and metal[11] nanoparticles by AFM has recently been demonstrated.

AFM was performed on the NC samples after transfer to the microscope enclosure; a surface oxide layer was thus expected to be present on the nanocrystals. The degree of oxidation was evaluated using x-ray photoemission spectroscopy performed on 15 nm Si NCs deposited on a Ge substrate. Si $2p$ core level analysis showed a substantial unshifted Si peak after 2 h of ambient exposure, indicating an oxide shell thickness of <3 nm. Oxidation of the AFM samples was minimized by storing the samples in flowing nitrogen; the AFM enclosure was also purged with nitrogen during data acquisition.

Since Si NCs are of great interest as charge storage nodes in NVM devices, the goal of this work was not only to demonstrate nondestructive imaging but also to perform charge injection into a NC and monitor its discharge using AFM. Single-electron transport through Si NCs has recently been observed.[12] In other work,[13] charging was performed on buried arrays of Co nanoclusters. The goal of the experiments described here was to accomplish charging of isolated

[a]Also at: Jet Propulsion Laboratory, California Institute of Technology, Pasadena, CA 91109; electronic mail: dbell@vaxeb.jpl.nasa.gov

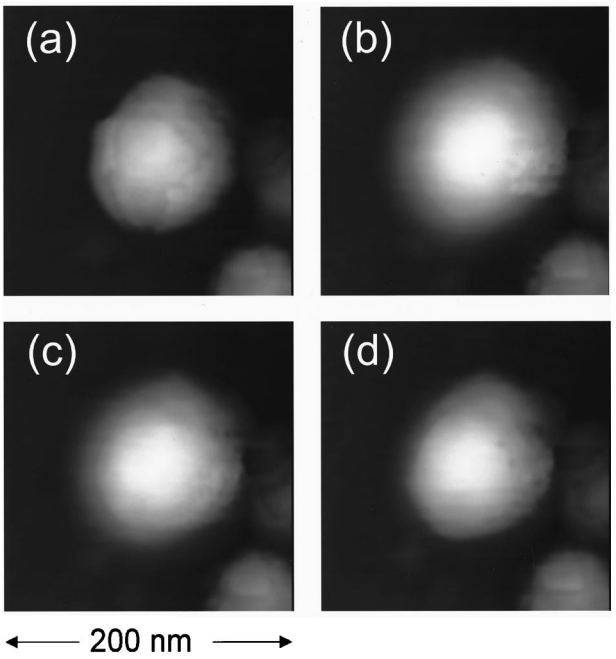

FIG. 1. AFM images of the charging and discharging of a single Si NC. Nanocrystal size (height) as measured by AFM is about 28 nm. Imaged area in each panel is 200×200 nm. (a) NC before charging. (b), (c), (d) images acquired at 45, 217, and 527 s after charging.

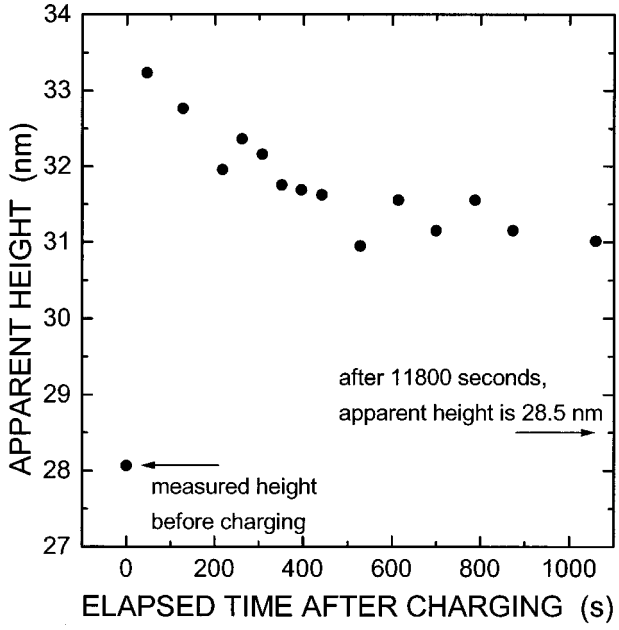

FIG. 2. Apparent NC height before charging by AFM and during discharging. Heights were measured from a series of AFM images of a single nanocrystal. The images shown in Fig. 1 were taken from the same series.

Si NCs on an insulating substrate. In this way individual NC electronic properties may be probed, and electron injection parameters can be more precisely controlled. Effects of oxide thickness and surface properties can also be studied on the single NC level. In addition, charging of bulk oxide defects, which could contribute for NCs buried within oxide layers, can be ruled out.

The presence of excess charge in the NC produces an electrostatic contribution to total force between AFM tip and sample. The AFM feedback causes the tip to retract to maintain the requested oscillation amplitude, and the charging manifests as an increase in apparent height in an AFM image.

To perform NC charging, the AFM tip was halted directly over a NC, a voltage was applied, and the average tip-sample distance was decreased from tapping-mode distance to the point where measurable charge could be transferred. Average distance was controlled by monitoring the attenuation of the AFM cantilever oscillation amplitude. The tip was held at the desired position for a short time (usually 30 s) after which it was retracted for tapping mode imaging. Applied tip voltage during charging was -20 V.

Charging experiments were performed in flowing gaseous nitrogen. In addition to slowing the oxidation of the NC, the nitrogen environment served to minimize water exposure. The presence of water vapor in room air was found to greatly decrease the discharge time of NC samples made by ion implantation of SiO_2 films, suggesting that an adsorbed water layer provided a conduction path for the discharge process. This decrease in discharge time was found to be reversible upon reintroduction of those samples into nitrogen.

Figure 1 shows several sequential AFM images of a charged Si NC, taken from a larger series of image data. The apparent lateral diameter of the NC in the AFM images reflects the tip radius of curvature, nominally 25–50 nm, but height AFM measurements indicate a NC diameter of about 28 nm. These sequential images show the initial increase [Fig. 1(b)] and subsequent decrease [Figs. 1(c) and 1(d)] in the stored charged with time, indicated by a change in apparent height and lateral diameter. This apparent change in height indicates that the AFM is sensitive to the injected charge. Resolution is observed to degrade when the NC is charged (also apparent in Fig. 1) due to the long-range nature of the electrostatic force compared with the short-range repulsive force that contributes in tapping-mode imaging. The apparent heights for this NC data set are plotted in Fig. 2. It can be seen that an increase in apparent height of about 5 nm occurs initially, and that after 1000 s the NC has only partially discharged.

Although additional observations of the charging/discharging process were made, there were cases for which no charging effect was seen. This was possibly due to excessive oxidation of the NC, prior contamination of the tip, accelerated discharging of the NC due to the presence of contamination or defects, or insensitivity to the small quantity of charge injected. Charging and discharging have been observed in NCs as small as 4 nm, with an apparent height change due to charging of only about 1 nm.

A model of the response of the AFM tip to fixed charge was developed. The electrostatic force on the tip due to the charged NC was calculated by first assuming a uniform surface charge over the upper half of the nanocrystal then using the method of images to find the induced image charge in the tip. The Coulomb interaction between these two charge distributions was then calculated to determine the total electrostatic force between tip and sample. The tip's motion as a function of time was solved from the equation for a simple harmonic oscillator

$$m\ddot{z}+\gamma\dot{z}+k(z-z_0)=F_0\cos(\omega t)+(F_{\text{tip–sample}})_z, \qquad (1)$$

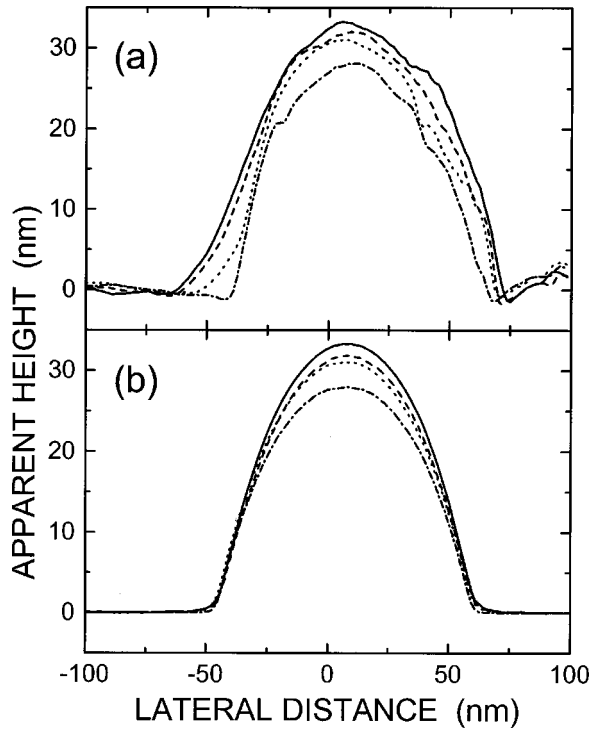

FIG. 3. (a) Measured and (b) calculated apparent NC heights for several different values of excess charge. Calculated profiles are shown for (from bottom) 0e, 41e, 45e, and 53e charges on the nanocrystal.

where tip mass ($m=10^{-11}$ kg), damping constant ($\gamma=10^{-11}$ kg), spring constant ($k=2.16$ N/m), driving force ($F_0=0.48$ nN), and driving frequency ($\omega=2\pi f, f=73.13$ kHz) were estimated from experiments or tip manufacturer's specifications. The term representing the force interaction between the tip and sample, $(F_{\text{tip-sample}})_z$, had three components: one due to the van der Waals' force when the tip is not in contact with the sample,[14] another representing the contact forces,[15] and the third representing the electrostatic term. The tip oscillation amplitude decreases approximately linearly with tip-sample spacing when the tip taps the surface. Model image contours can be generated by adjusting the average tip-sample spacing in the model (i.e, z_0) to maintain a constant set-point amplitude (in this case 10.3 nm). The resulting calculated ''image'' is the set of average tip heights (z_0) maintained by the tip as it scans over the charged particle, with a constant set-point oscillation amplitude. Further details of this model will be given in a future publication; however, modeling indicates that the results do not depend strongly on the assumed nature of the contact force, and charge resolution is of order a few electrons. This resolution was also found to depend somewhat on tip radius of curvature. Figure 3 shows the measured and calculated contours across the NC of Fig. 1 for several charge states. These calculations yield a maximum stored charge of order 50 electrons.

In conclusion, size-classified ensembles of Si NCs on insulating substrates have been formed using aerosol techniques. Conducting AFM tips have been used to inject charge into single Si NCs and to monitor the subsequent discharge. A model for the response of the AFM system to the electrostatic force produced by excess charge allows an estimate of the quantity of charge injected into the nanocrystals.

The research described in this paper was jointly sponsored by the National Aeronautics and Space Administration (NASA) and the Jet Propulsion Laboratory Director's Research and Development Fund, and by the National Science Foundation under Grant No. DMR 98-71850.

[1] K. Yano, T. Ishii, T. Hashimoto, F. Murai, and K. Seki, IEEE Trans. Electron Devices **41**, 1628 (1994).
[2] S. Tiwari, F. Rana, H. Hanafi, A. Hartstein, E. F. Crabbe, and K. Chan, Appl. Phys. Lett. **68**, 1377 (1996).
[3] L. Guo, E. Leobandung, and S. Y. Chou, Science **275**, 649 (1997).
[4] H. I. Hanafi, S. Tiwari, and I. Khan, IEEE Trans. Electron Devices **43**, 1553 (1996).
[5] R. P. Camata, H. A. Atwater, K. J. Vahala, and R. C. Flagan, Appl. Phys. Lett. **68**, 3162 (1996).
[6] J. J. Wu, H. V. Nguyen, and R. C. Flagan, Langmuir **3**, 266 (1987).
[7] G. Binning, C. F. Quate, and Ch. Gerber, Phys. Rev. Lett. **56**, 930 (1986).
[8] Y. Martin, D. W. Abraham, and H. K. Wickramasinghe, Appl. Phys. Lett. **52**, 1103 (1988).
[9] Q. Zhong, D. Inniss, K. Kjoller, and V. B. Elings, Surf. Sci. **290**, L688 (1993).
[10] T. Junno, K. Deppert, L. Montelius, and L. Samuelson, Appl. Phys. Lett. **66**, 3627 (1995).
[11] T. R. Ramachandran, C. Baur, A. Bugacov, A. Madhukar, B. E. Koel, A. Requicha, and C. Gazen, Nanotechnology **9**, 237 (1998).
[12] M. Otobe, H. Yajima, and S. Oda, Appl. Phys. Lett. **72**, 1089 (1998).
[13] D. M. Schaadt, E. T. Yu, S. Sankar, and A. E. Berkowitz, Appl. Phys. Lett. **74**, 472 (1999).
[14] H. C. Hamaker, Physica (Amsterdam) **IV**, 1058 (1937).
[15] K. L. Johnson, K. Kendall, and A. D. Roberts, Proc. R. Soc. London, Ser. A **324**, 301 (1971).